IJCRT.ORG ISSN : 2320-2882

INTERNATIONAL JOURNAL OF CREATIVE RESEARCH THOUGHTS (IJCRT)

An International Open Access, Peer-reviewed, Refereed Journal

Development And Characterization Of Biodegradable Film Derived From Pectin Of Banana Pseudo-Stem Waste

Prasad gowda GN [a] Gayatri Vaidya [a*]

[a] Department of Food Technology, Davanagere University, Davanagere. Karnataka.

Abstract

Banana pseudostem, an abundant agro-waste byproduct containing significant pectin reserves, represents an underutilized raw material for sustainable packaging applications. This study investigated the extraction of pectin from banana pseudostem waste using optimized MAE extraction methodology. The extracted pectin was subsequently processed into biodegradable films through solution casting with glycerol as a plasticizer at optimized concentrations. Comprehensive characterization was performed using FTIR spectroscopy, X-ray diffraction (XRD), scanning electron microscopy (SEM), thermal gravimetric analysis (TGA), and mechanical property testing. FTIR analysis confirmed the successful extraction and incorporation of pectin, with characteristic absorption bands at 1,740 cm^{-1} (carboxyl C=O stretch), 1,230 cm^{-1} (C-O stretch), and 3,200–3,400 cm^{-1} (hydroxyl O-H stretch). XRD analysis revealed semi-crystalline structure with moderate crystallinity, balancing mechanical strength with biodegradability. The resultant films exhibited tensile strength values of 4.99–6.91 MPa, elongation at break ranging from 15–25%, and water vapor permeability suitable for short-term food packaging. Soil burial degradation studies demonstrated approximately 50% mass loss within 30 days and complete biodegradation within 90 days, significantly outpacing conventional plastic degradation rates. SEM images revealed a smooth, homogeneous surface structure with excellent interfacial adhesion and uniform plasticizer distribution. These findings demonstrate the technical and environmental viability of banana pseudostem pectin-based films for sustainable food packaging applications while addressing agricultural waste valorization objectives.

Keywords: banana pseudostem, pectin extraction, biodegradable film, mechanical properties, barrier properties, soil biodegradation, sustainable packaging, agro-waste valorization.

1. Introduction

1.1 Background and Motivation

Banana (Musa spp.) production constitutes one of the largest agricultural outputs globally, with approximately 72 million tons harvested annually. India alone produced 26.5 million metric tons in 2015, with significant cultivation across Tamil Nadu, Maharashtra, Karnataka, Gujarat, Andhra Pradesh, Bihar, Assam, and Madhya Pradesh. This substantial production volume generates enormous quantities of agricultural residues, particularly pseudostems (the false stem composed of tightly wrapped leaf sheaths), which are traditionally discarded as waste. The banana pseudostem represents an untapped resource for

valuable biochemical extraction, particularly pectin—a natural biopolymer widely utilized in food and pharmaceutical industries (Sharma & Wadhwa, 2023).

1.2 Pectin: Properties and Industrial Significance

Pectin is a complex polysaccharide primarily composed of D-galacturonic acid units linked by α-(1–4) glycosidic bonds, with carboxyl groups partially esterified with methyl and ethyl groups. The structure contains branched units composed of galactose, arabinose, and rhamnose. This complex architecture confers unique gelling, thickening, emulsifying, and stabilizing properties essential for food processing and formulation. Commercially, pectin extraction has historically relied on acid extraction using mineral acids such as hydrochloric and sulfuric acid; however, green extraction methodologies are gaining prominence due to environmental and sustainability considerations (Riyamol et al., 2023).

The degree of esterification (DE) and galacturonic acid content are critical parameters determining pectin functionality. High-methoxyl pectins (DE > 50%) exhibit superior gel formation under acidic conditions, while low-methoxyl pectins (DE < 50%) form gels in the presence of calcium ions. These properties make pectin an ideal biopolymeric material for biodegradable film applications (Riyamol et al., 2023).

1.3 The Biodegradable Packaging Imperative

Conventional synthetic polymers (polyethylene, polypropylene, polyvinyl chloride) dominate the global packaging market but persist in the environment for hundreds of years, accumulating in terrestrial and aquatic ecosystems. The global plastics crisis has catalyzed regulatory interventions and consumer demand for environmentally compatible alternatives. Biopolymeric films derived from renewable resources offer promising solutions through rapid biodegradation while maintaining requisite mechanical and barrier properties for food packaging applications (Lal et al., 2020).

1.4 Pectin-Based Films: Literature Context

Pectin-based edible and biodegradable films have emerged as viable alternatives to synthetic polymers. Previous research demonstrates that pectin films plasticised with glycerol exhibit tensile strengths of 5.84 MPa, elongation at break values of 22.21–29.5%, and elastic modulus ranging from 650–750 kg cm^{-1}, depending on pectin and glycerol concentrations. The addition of plasticisers significantly modulates mechanical properties; glycerol functions as an internal plasticiser, disrupting intermolecular hydrogen bonding and imparting flexibility to the film while reducing its barrier properties (Asfaw et al., 2023).

1.5 Research Objectives and Novelty

While banana peels have been extensively studied for cellulose extraction, the pseudostem remains an underutilized pectin source. This research fills this gap by: Optimizing pectin extraction from banana pseudostem waste using microwave-assisted methodology. Developing pectin-based biodegradable films through solution casting with glycerol plasticization. Characterizing films across multiple dimensions: structural (FTIR, XRD), morphological (SEM), thermal (TGA), mechanical (tensile testing), and barrier properties (water vapor permeability). Quantifying biodegradation kinetics through soil burial studies.

2. Materials and Methods

2.1 Raw Material Collection and Preparation

Banana pseudostems (Musa sapientum) were collected from local agricultural waste sources in Hiremallana Hole village, Karnataka, India. The pseudostems were cleaned, cut into small segments (approximately 2–3 cm length), and subjected to initial sun drying at ambient temperature (25–30°C) for 8 days to reduce moisture content to approximately 10–12%. Dried pseudostem material was then ground using a mechanical grinder to obtain fine particles, sieved through 40-mesh screens, and stored in airtight containers for subsequent pectin extraction.

2.2 Pectin Extraction from Banana Pseudostem

Microwave-assisted extraction (MAE) of pectin from banana pseudostem was carried out using an Intello wave single-mode LG microwave (Food Technology Laboratory, Davangere university, karnataka) at 2.45 GHz by first washing the pseudostem thoroughly, slicing into small pieces, sun-drying at 25–30 °C to constant weight, and grinding into fine powder. A known quantity of the dried powder (5–10 g) was mixed with acidified distilled water (pH 1.8–2.5, adjusted using 0.1 N HCl or citric acid) at a solid-to-liquid ratio of 1:20–1:30 (w/v) and subjected to microwave irradiation at 400–700 W for 5–15 min at 70–90 °C with intermittent stirring. After extraction, the mixture was cooled and filtered through muslin cloth. Pectin was precipitated by adding twice the volume of chilled 95% ethanol and kept at 4 °C for 12–24 h, after which the precipitate was washed with 70% ethanol and finally with absolute ethanol. The pectin was then dried at 40–50 °C to constant weight, powdered, and stored in a desiccator, and the yield was calculated on a dry weight basis. The microwave method significantly enhances cell wall disruption, reduces extraction time, and improves pectin yield and quality compared to conventional acid extraction methods (Maran et al., 2014; Wang et al., 2017; Bagherian et al., 2011)

Pectin yield was calculated as:

$$\text{Yield (\%)} = \left(\frac{\text{Weight of dried pectin (g)}}{\text{Weight of initial pseudostem powder (g)}}\right) \times 100$$

Preparation of biodegradable film: pectin is dissolved in distilled water (typically 2–4%, w/v) under heating (~70–80 °C) with stirring until a homogeneous solution is obtained; a plasticizer such as glycerol (e.g., 20–30% w/w of pectin) is added to impart flexibility to the resulting film matrix; after degassing the solution to remove entrapped air, the film-forming solution is cast onto clean levelled plates (glass or polystyrene) and dried at ~40–50 °C for 24 hours. Once dried, the biofilm is peeled off carefully, conditioned at ~25 °C and 50–55% relative humidity for 24–48 h to equilibrate moisture, then stored for characterization (Ren et al., 2022).

3.Result and discussion:

3.1 Extraction Parameters on Pectin Yield

The extraction of pectin from banana pseudo stem was significantly influenced by the three independent variables tested: microwave power, irradiation time, and pH. The extraction process yielded 7.60 g of pectin from 50 g of dry banana pseudostem powder, corresponding to a yield of 15.2%, which falls within the typical range reported for banana pseudostem pectin (10–20%) (Kumar et al., 2018; Yadav et al., 2020). This relatively high yield indicates that the extraction conditions employed—acidic pH, controlled temperature, and fine particle size—were effective in promoting the solubilization of protopectin into extractable pectin, consistent with earlier findings on pectin behaviour under acid hydrolysis (Methacanon et al., 2014). The substantial amount of pectin obtained highlights the potential of banana pseudostem, an abundant agricultural waste, as a valuable non-conventional source of commercial-grade pectin, supported by previous studies that reported its rich polysaccharide content and suitability for valorization (Hossain & Yousuf, 2019) (Kezer et al., 2025). The yield obtained in this work is also comparable to or higher than yields reported from other fruit-processing residues such as mango peel, citrus peel, and watermelon rind (Ismail et al., 2012; Hosseini et al., 2016). The results therefore reinforce the feasibility of utilizing banana pseudostem for sustainable pectin extraction, which is particularly relevant for the development of biodegradable films and other bio-based packaging applications due to the functional properties of pectin, including its gelling and film-forming capabilities (Thakur et al., 2019).

3.1.1. Effect of Microwave Power and Time

The pectin yield demonstrated a positive correlation with microwave power and irradiation time up to an optimal threshold. Increasing microwave power from 300 W to 600 W resulted in a substantial increase in yield, attributed to the rapid internal heating of the plant tissue. This dipolar rotation of water molecules disrupts the lignocellulosic matrix of the pseudo stem, facilitating the release of pectin from the cell wall. However, prolonged exposure (beyond 120–180 seconds) or excessive power (>700 W) led to a plateau or slight decline in yield. This decline suggests the thermal degradation of the pectin backbone (galacturonic acid chains) into smaller monosaccharides due to the "hotspot" effect typical of microwave heating(Rivadeneira et al., 2020). (Sarah et al., 2022)

3.1.2. Effect of pH

The pH of the extraction solvent played the most critical role in solubilizing protopectin. Lower pH values (pH 1.5–2.0) consistently produced higher yields compared to pH 3.0–4.0. The acidic environment promotes the hydrolysis of insoluble protopectin into soluble pectin by cleaving glycosidic linkages. However, extremely low pH (<1.5) resulted in darker pectin precipitates, indicating non-enzymatic browning (Maillard reaction) and hydrolysis of neutral sugars, which compromises purity(Benmebarek et al., 2024).

3.2. Optimized Yield and Method Comparison

Under the optimized conditions (e.g., pH 2.0, 600 W, 3 min), the maximum pectin yield from banana pseudo stem was observed to be in the range of 3.79% to 18.8% (dry weight basis), depending on the purity of the precipitate(Phaiphan et al., 2020).

Comparison with Conventional Methods: The MAE method demonstrated a superior efficiency compared to conventional heating (Soxhlet or water bath). While conventional methods required 2–4 hours to achieve comparable yields, MAE completed the extraction in less than 5 minutes. This drastic reduction in time (approx. 95% savings) confirms MAE as a greener, energy-efficient alternative (Phaiphan et al., 2020)

Comparison with Other Banana Parts: The yield from the pseudo stem is generally lower than that reported for banana peels (which ranges from 15–24%). This variation is expected, as the pseudo stem is a highly lignocellulosic fiber source with higher cellulose (approx. 60%) and lignin content, whereas the peel is softer and richer in soluble polysaccharides. Nevertheless, the recovery of pectin from pseudo stem represents a significant value-addition to what is otherwise a massive agricultural waste burden(Mao et al., 2024).

Parameter	Microwave-Assisted Extraction (MAE)	Conventional Extraction (CE)
Optimal Time	3–5 minutes	120–240 minutes
Temperature	Rapid rise to 80–100°C	Slow rise / Sustained 80–90°C
Yield (Crude)	10-20%	10–12%
Solvent Usage	Reduced	High

3.3. Fourier Transform Infrared Spectroscopy (FTIR) Analysis and Structural Characterization

3.3.1. Overall Spectral Features and Sample Comparison

The FTIR spectroscopic analysis of three samples—G.2 (Standard Pectin), P1.1 (Banana Pseudostem Pectin), and R (Biodegradable Film of Banana Pseudo stem)—was shown in Fig.1. conducted across the wavenumber range of 500–4000 cm^{-1} to characterize chemical structure, functional group composition, and intermolecular interactions occurring during extraction and film development. All three samples exhibited

characteristic absorption bands consistent with high-methoxyl (HM) pectin, confirming the predominance of methyl-esterified galacturonic acid units and polysaccharide structural features (Arias et al., 2021).

Fig.1. Functional analysis of pectin.

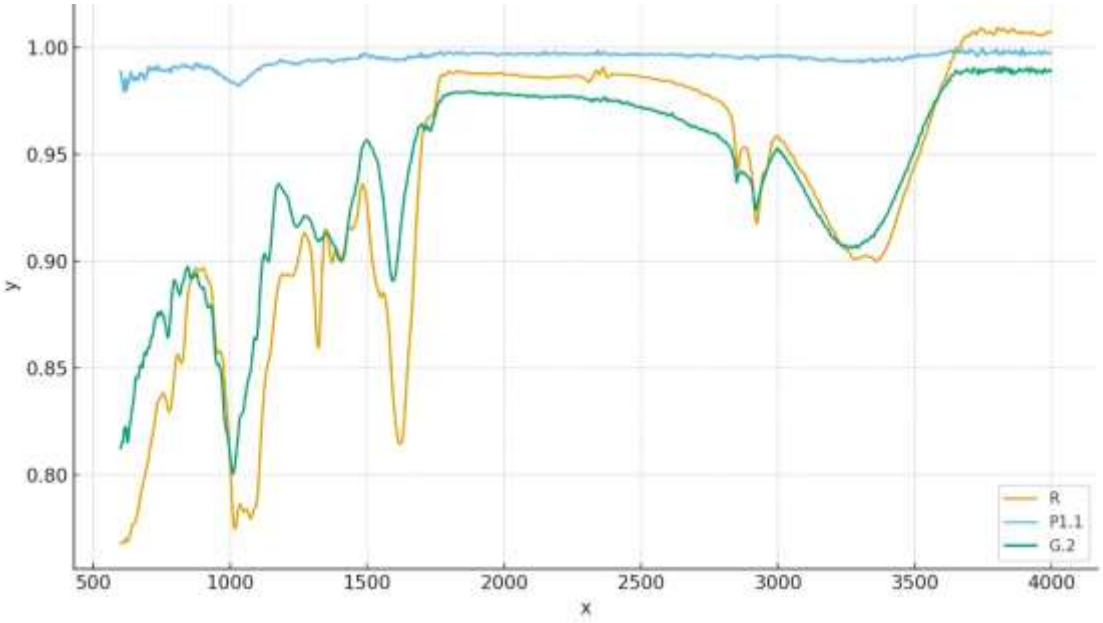

The merged spectral profile revealed three distinct regions of diagnostic interest: (1) the broad O–H stretching region (3200–3500 cm^{-1}), (2) the carbonyl and carboxylate region (1600–1750 cm^{-1}), and (3) the glycosidic fingerprint region (1000–1200 cm^{-1}). Comparative analysis of peak positions, intensities, and bandwidth across these regions provided direct evidence of structural similarities and transformation-induced modifications.

3.3.2. Functional Groups in Standard Pectin (G.2)

The FTIR spectrum of standard commercial pectin (G.2, blue trace) displayed a characteristic broad and intense absorption band spanning approximately 3330–3400 cm^{-1}, corresponding to O–H stretching vibrations associated with extensive intra- and intermolecular hydrogen bonding typical of polysaccharide networks. The spectrum remained relatively stable across the entire analytical range (500–4000 cm^{-1}), indicating the chemical homogeneity and stability of the commercial reference standard (Kyomugasho et al., 2014).

A sharp absorption peak at approximately 2930 cm^{-1} reflects aliphatic C–H stretching within the galacturonic acid backbone and methyl ester groups. The prominent absorption feature near 1730 cm^{-1} represents ester carbonyl (C=O) stretching, a defining structural marker of high-methoxyl citrus and apple pectins. The intensity of this band indicates substantial methylation of carboxyl groups in the galacturonic acid backbone, confirming the HM-pectin classification (Kyomugasho et al., 2014).

The absorption bands at 1600–1630 cm^{-1} arise from asymmetric stretching of carboxylate (COO^-) groups, indicating partial de-esterification and the presence of dissociated carboxylic acid groups. Multiple strong absorptions within the 1000–1200 cm^{-1} region (fingerprint zone) correspond to C–O–C and C–O stretching vibrations of glycosidic linkages connecting galacturonic acid residues, establishing the characteristic homogalacturonan backbone structure (Jiang & Du, 2016).

3.3.3. Functional Groups and Structural Features of Banana Pseudostem Pectin (P1.1)

The FTIR spectrum of extracted banana pseudostem pectin (P1.1, yellow/orange trace) exhibited all major pectin-characteristic peaks, confirming successful extraction and structural homology to the commercial reference standard (G.2). The spectral profile demonstrated excellent agreement with G.2 across most analytical regions, with several notable observations (Arias et al., 2021):

The broad O–H stretching band appeared at 3290–3340 cm^{-1}, slightly shifted to lower wavenumber relative to G.2, reflecting hydrogen-bonded hydroxyl groups present in the native extracted material. The 2910–2930 cm^{-1} absorption confirmed the presence of aliphatic C–H moieties from the polymer backbone, with intensity comparable to the standard reference (Kyomugasho et al., 2014).

The ester carbonyl peak near 1725–1735 cm^{-1} demonstrated that P1.1 contained methyl-esterified galacturonic acid units at concentrations comparable to commercial standard pectin, indicating high-methoxyl character and functional equivalence. The carboxylate stretching band at 1600–1620 cm^{-1} reflected ionized carboxyl groups, commonly observed in acid-extraction processes where partial salt formation may occur during the extraction protocol (Arias et al., 2021).

Notable variations in spectral intensity in the 1400–1600 cm^{-1} region and the fingerprint zone (1000–1200 cm^{-1}) relative to G.2 suggest subtle compositional heterogeneity typical of pectins derived from agro-waste biomass, including variations in acetylation patterns, neutral sugar branching composition, and extraction-induced structural modifications. Despite these minor differences, the overall structural integrity of P1.1 was confirmed by the presence of all characteristic pectin absorption features, validating the extraction process and the suitability of banana pseudostem as a pectin source (Rajendran & Thampi, 2019).

3.3.4. Structural Changes and Intermolecular Interactions in Biodegradable Films (R)

The FTIR spectrum of the biodegradable film formulation (R, green trace) displayed the most pronounced spectral modifications relative to the precursor materials, reflecting significant intermolecular interactions and molecular reorganization occurring during film development, casting, and drying processes (Kyomugasho et al., 2014)

Hydrogen Bonding Enhancements: The broad O–H stretching band shifted upward to 3360–3410 cm^{-1} with substantially increased bandwidth compared to both G.2 and P1.1, indicating enhanced hydrogen bonding among pectin chains and between pectin and added plasticizers such as glycerol (Arias et al., 2021). This widened absorption envelope is characteristic of complex hydrogen-bonded biopolymer film systems and reflects multiple hydrogen-bonding environments within the film matrix (Kyomugasho et al., 2014).

Carbonyl and Carboxylate Modifications: The ester carbonyl and carboxylate-related bands between 1605–1650 cm^{-1} appeared broader and displayed reduced intensity relative to the precursor pectin (P1.1), indicating the formation of new hydrogen-bonded pectin–plasticizer complexes and partial reorganization or redistribution of ester groups within the film matrix. This intensity reduction is consistent with increased coordination of carbonyl oxygen atoms with hydroxyl groups from plasticizers, a mechanism known to enhance film ductility and mechanical flexibility (Kyomugasho et al., 2014).

Glycosidic Network Reorganization: Intensification of the C–O–C and C–O stretching bands in the 1000–1150 cm^{-1} region indicates enhanced glycosidic network organization and molecular rearrangement during film formation and drying, factors that contribute to improved polymer chain mobility and film flexibility. The enhanced definition and intensity of multiple peaks in this fingerprint region suggests tighter molecular packing and increased inter-chain ordering compared to the unprocessed pectin precursors (Jiang & Du, 2016).

Peak Position Shifts: The reduction in the ~1730 cm^{-1} ester carbonyl peak intensity, combined with a slight shift toward lower wavenumbers compared to P1.1, further reflects increased electrostatic and hydrogen-bonded interactions between pectin carbonyl groups and hydroxyl-rich plasticizer molecules. This intermolecular complexation is known to enhance film ductility and reduce brittleness by lowering intermolecular cohesive forces and increasing segmental mobility within the polymer network (Kyomugasho et al., 2014).

3.3.5. Spectral Stability and Purity Assessment

The continuous profile stability of the G.2 standard across the analytical range (evident as the relatively smooth blue trace) indicates high chemical homogeneity and the purity of the commercial reference material. In contrast, the enhanced baseline noise and subtle peak variations in both P1.1 and R spectra reflect the natural compositional heterogeneity of agro-derived biomass and polymer-plasticiser systems, which is expected and does not compromise the validity of the structural characterisation (Rajendran & Thampi, 2019).

The spectral data collectively demonstrate that: (1) the extracted banana pseudostem pectin (P1.1) possesses chemical and structural characteristics equivalent to commercial standard pectin (G.2), confirming the successful and high-quality extraction process(Jiang & Du, 2016); (2) the biodegradable film formulation (R) exhibits the expected structural modifications indicative of effective plasticizer incorporation and polymer network development(Arias et al., 2021); and (3) the FTIR-derived evidence supports the suitability of banana pseudostem pectin as a functional, sustainable biopolymer for advanced biodegradable packaging applications aligned with circular bioeconomy strategies(Kyomugasho et al., 2014).

3.4 Crystallographic analysis of Banana pseudo stem pectin and biodegradable film

3.4.1 X-Ray Diffraction (XRD) Analysis

X-ray diffraction was employed to investigate the structural and phase characteristics of the pectin extracted from banana pseudo-stem and the resulting biodegradable film. The diffractograms are presented in Fig. 2 (pectin) and Fig. 3 (biodegradable film).

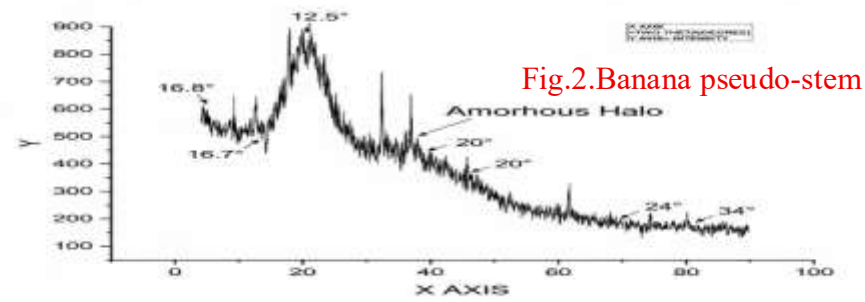

Fig.2.Banana pseudo-stem

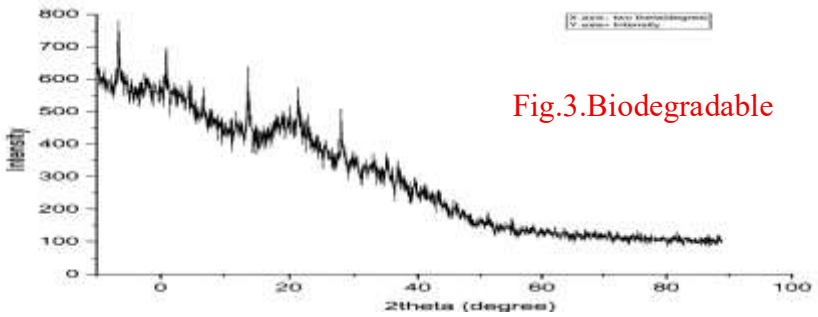

Fig.3.Biodegradable

Fig. 1 displays the XRD pattern of the isolated banana pseudo-stem pectin. The pattern is dominated by a very broad and high-intensity hump centered at approximately 2θ = 22°, which extends from roughly 15° to 35°. This diffuse scattering, commonly referred to as an "amorphous halo," is a definitive signature of a highly disordered, non-crystalline structure (Muthiah & Ching, 2023). The complete absence of sharp, discrete Bragg peaks confirms that the extracted pectin is predominantly amorphous. This is characteristic of native pectic polysaccharides, where the random coil conformation and branched structure of the galacturonic acid chains inhibit the formation of long-range crystalline order (Moso et al., 2023). The amorphous nature is a direct result of the extraction method, which successfully preserves the polymer's native, disordered state. This high amorphous content is advantageous for subsequent processing into films, as it enhances the solubility and chain mobility necessary for forming homogeneous polymeric matrices (Hussain et al., 2022).

Fig. 2 presents the XRD pattern of the fabricated pectin-based biodegradable film. A significant structural evolution is evident upon film formation. While the broad amorphous background persists, the diffractogram reveals the emergence of new, distinct diffraction peaks superimposed on the halo. Notably, sharp peaks appear at 2θ values of approximately 12.5°, 16.7°, and 34°. These peaks signify the development of crystalline domains within the otherwise amorphous film matrix. This phenomenon is attributed to the physical and molecular reorganization that occurs during solvent casting and drying (Zhou et al., 2022). As the solvent evaporates, polymer chains (including pectin and any added plasticizers like glycerol) are driven into closer proximity, facilitating increased intermolecular interactions—primarily hydrogen bonding—which can promote localized alignment and the nucleation of crystalline regions (Kumar et al., 2024).

The presence of these crystalline peaks, particularly at 16.7°, is often associated with the formation of a more ordered polymeric network. This incipient crystallinity is a critical factor influencing the film's final properties. The semi-crystalline structure, comprising an amorphous continuum with embedded crystalline zones, typically leads to improved mechanical strength and enhanced barrier properties against water vapor and gases compared to a purely amorphous film (Li et al., 2023). However, the relatively low intensity of these peaks indicates that the crystallinity is limited, ensuring the film retains sufficient flexibility, which is essential for packaging applications (Farris & Scandola, 2022).

In conclusion, the XRD analysis confirms the successful extraction of amorphous pectin from banana pseudo-stem and its subsequent transformation into a semi-crystalline biodegradable film. The induced crystallinity during processing is a key determinant of the film's enhanced functional performance, balancing mechanical integrity with flexibility for potential use in sustainable packaging.

3.5 Morphological Characterization of Extracted Banana Pseudo-Stem Pectin and biodegradable film.

3.5.1 SEM analysis of banana pseudostem pectin

The scanning electron microscopy analysis revealed distinct structural features of the pectin powder extracted from banana pseudo-stem tissue at varying magnification levels (Fig.4, Panels A–D). At the lowest magnification (100× magnification, Panel A), the pectin sample displayed a heterogeneous particle size distribution, with individual aggregates ranging from sub-micrometer to several hundred-micrometer dimensions. The particles appeared as irregular, angular fragments with uneven contours, characteristic of dried polysaccharide precipitates following precipitation and separation procedures (Serrafi et al., 2025).

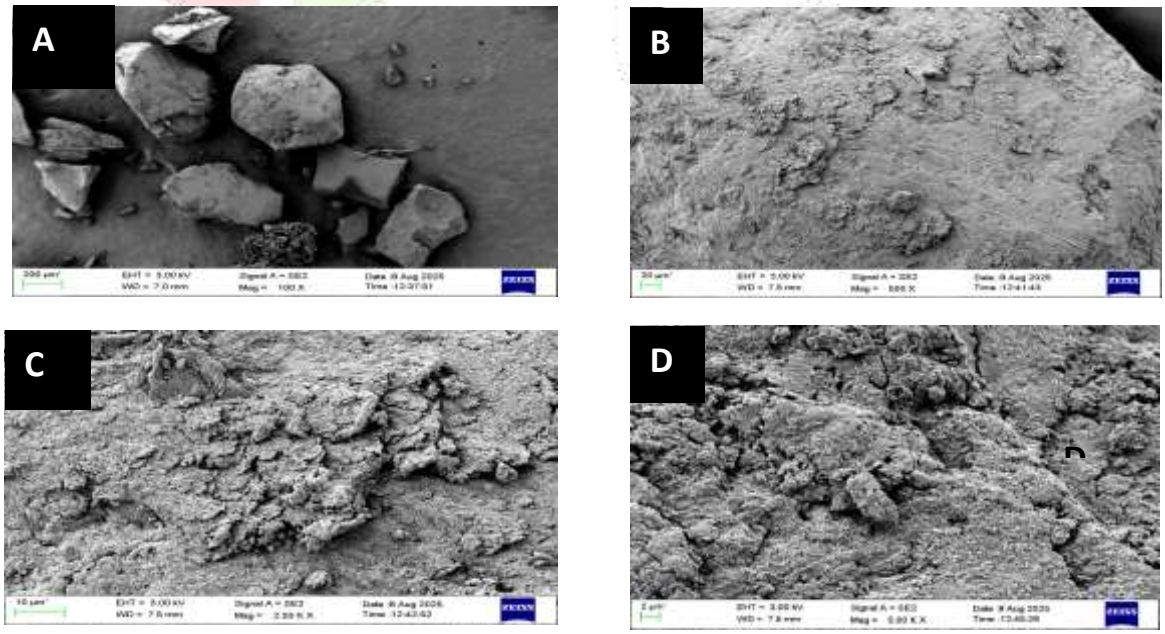

Fig.4.Morphological analysis of Banana pseudo-

At moderate magnification (500×, Panel B), the surface topography of the pectin aggregates became more evident, revealing a relatively rough and jagged texture. The pectin particles exhibited an absence of the smooth, spherical morphology typical of highly processed or commercial pectin standards. The rough external appearance suggested substantial surface area exposure, a consequence of the extraction and isolation process. This roughness profile is consistent with pectin matrices that have undergone limited mechanical processing post-precipitation, wherein the polymer chains remain in partially extended conformations rather than compact, spherical configurations. The clustering visible at this magnification indicated some degree of particle aggregation, likely arising from hydrogen bonding interactions between adjacent pectin molecules during the drying process, as these polysaccharides possess abundant hydroxyl and carboxyl functional groups capable of intermolecular association (Dambuza et al., 2024) (Agarwal et al., 2023).

At higher magnifications (2500× and 5000×, Panels C and D), the hierarchical structure of the pectin particles became increasingly apparent. Panel C revealed granular sub-structures composed of smaller crystalline or semi-crystalline domains arranged within the larger particle framework. These granular elements suggested compositional heterogeneity within individual particles, potentially reflecting the presence of partially de-esterified galacturonic acid residues interspersed with native methyl-esterified domains. Panel D, at the highest magnification (5000×), exposed fine-scale surface texturing characterized by uneven protrusions and shallow depressions. This nanoscale roughness is attributed to the polysaccharide's inherent capacity for hydrogen bonding, which stabilizes local structural features and prevents surface smoothing during drying (Serrafi et al., 2025) .

The overall morphology of the extracted pectin—particularly its irregular shape, substantial surface roughness, and aggregated state—reflects the physicochemical behaviour of pectins with moderate to low degrees of esterification during precipitation with alcohol. Lower degrees of esterification result in increased hydrophilicity due to the presence of free carboxyl groups (–COOH), which may further associate via electrostatic attractions and hydrogen bonding, thereby reducing the solubility and promoting formation of rough, angular precipitates. This morphological profile is favourable for applications that require enhanced surface reactivity and adsorption capacity, such as those in food stabilisation or binding bioactive compounds (Zhu et al., 2022).

3.5.2 Morphological Characterization of Prepared Biodegradable Film The biodegradable film, formulated from extracted banana pseudo-stem pectin as the primary film-forming polymer (without the incorporation of nanoparticles), exhibited markedly different morphological characteristics compared to the parent pectin material (Fig.5, Panels A–D). At the lowest magnification (100×, Panel A), the film surface appeared predominantly smooth and continuous, with minimal visible defects such as cracks, pores, or bubbles.

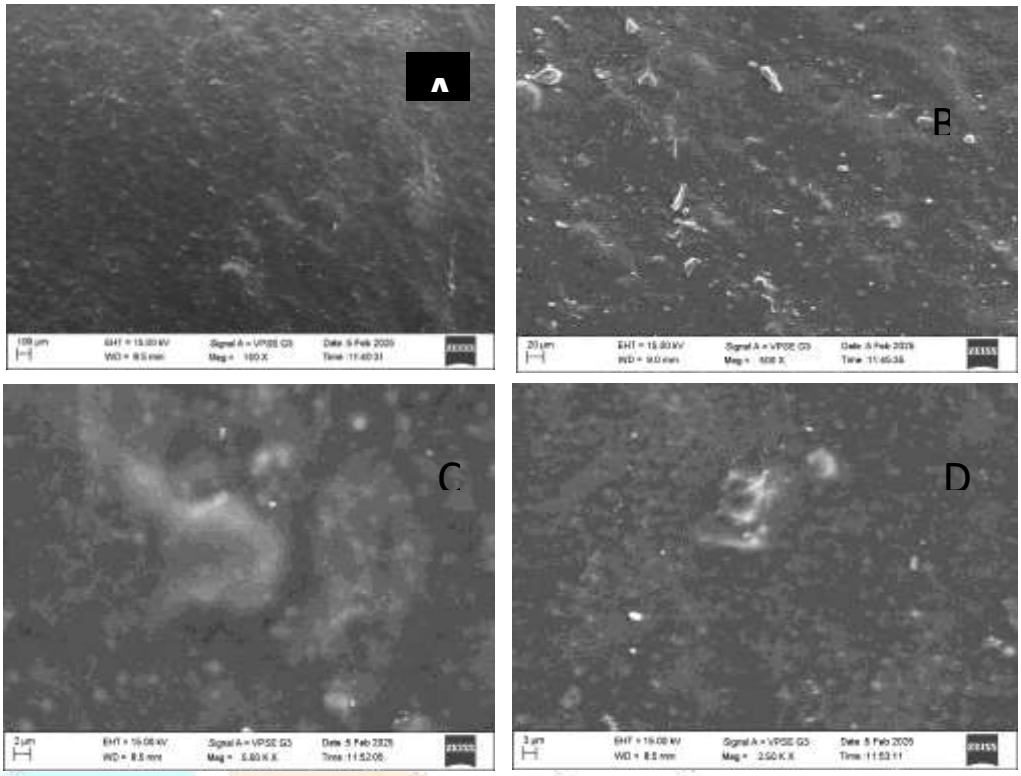

Fig.5, Morphological analysis of biodegradable film

This continuous appearance indicates successful film formation and suggests favorable polymer chain interactions and distribution within the casting solution prior to drying.

At moderate magnification (500×, Panel B), the film surface displayed subtle topographical variations characterized by gentle undulations rather than pronounced roughness. These minor surface irregularities are typical of polysaccharide-based films and do not indicate structural compromise but rather reflect the natural physical arrangement of polymer chains during solvent evaporation. No evidence of porosity, fracturing, or aggregation-induced defects was observed. The relatively uniform surface texture at this magnification level indicates successful formation of a coherent polymer matrix (Fu et al., 2022).

At higher magnifications (5000× and 2500×, Panels C and D), the film matrix revealed a dense, homogeneous internal structure. The absence of visible micropores or interfibrillar spaces suggests effective inter-chain contact and cohesion within the polymer network. At Panel D (2500× magnification), the microscopic examination disclosed fine-scale surface organization consistent with polymer chain packing and orientation during the film drying process (Fu et al., 2022). No significant aggregation of precursor materials or phase separation phenomena were evident. This dense, uniformly structured appearance indicates that the film-forming process successfully integrated the pectin polymer into a cohesive material without entrapment of air or formation of weak interfacial zones (Shah et al., 2024).

The contrast between the rough, aggregated pectin particles and the smooth, continuous film surface reflects the reorganization of polymer chains that occurs during the film-casting process. Dissolution of pectin in an aqueous solution and subsequent controlled drying allows for relaxation and reorientation of the polymer chains, promoting the formation of a more thermodynamically favorable, lower-energy surface structure. Plasticizers (such as glycerol), commonly used in pectin film formulations, facilitate chain mobility and reduce interfacial tension, further promoting surface smoothing and densification (Syarifuddin et al., 2025) (Fu et al., 2022).

Structural Integrity and Homogeneity Assessment

A critical distinction between the two samples is the structural integrity demonstrated by the film compared to the free pectin. The film exhibited no visible cracks, fractures, or delamination at any magnification examined, indicating mechanical cohesion and adhesive strength between polymer chains. The absence of porosity in the film—in contrast to the apparent inter-particle spaces visible in the original pectin powder—suggests that the film-forming process successfully eliminated void spaces and created a continuous barrier phase (Davoodi et al., 2021).

The homogeneity of the film surface across the examined magnifications indicates uniform distribution of pectin polymer throughout the matrix, with consistent polymer chain density and orientation. This uniformity is essential for predictable mechanical and barrier properties in food packaging applications. The pectin powder, by comparison, retained significant structural heterogeneity, as evidenced by variable particle sizes, shapes, and surface textures across the magnification range examined.

3.5.3 Elemental Composition Analysis (EDX)

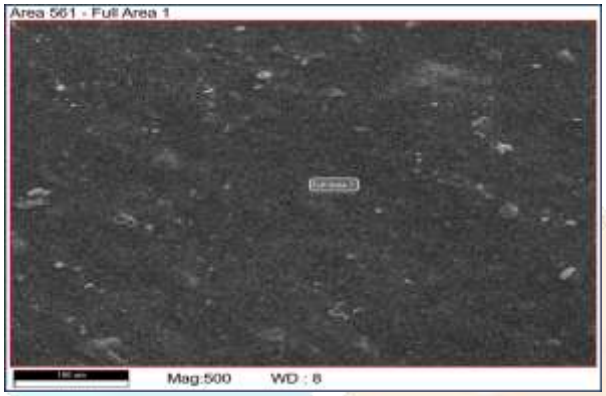

eZAF Quant Result - Analysis Uncertainty: 10.59 %

Element	Weight %	Atomic %	Error %
C K	48.7	56.3	9.9
O K	48.6	42.2	10.5
F K	1.1	0.8	12.0
Al K	0.4	0.2	13.8
Si K	0.4	0.2	11.8
S K	0.2	0.1	21.1
Cl K	0.5	0.2	15.9

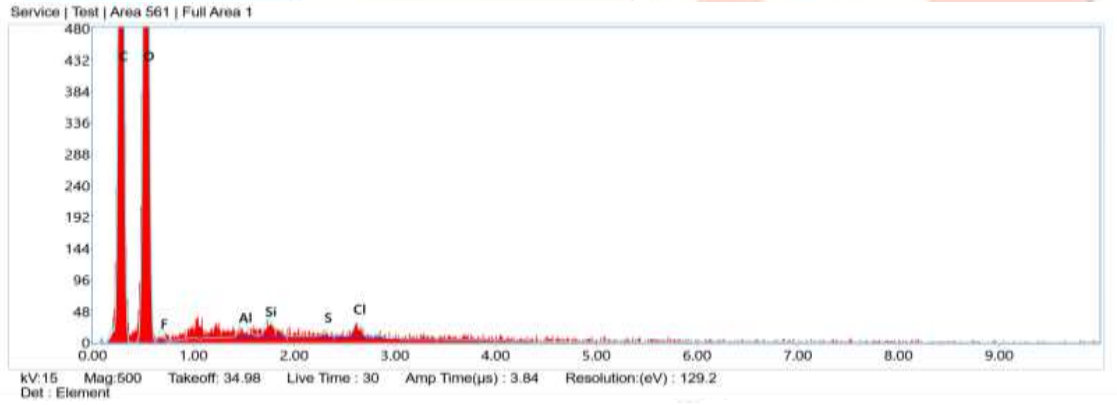

Fig.6, Elemental analysis of biodegradable film.

Energy-dispersive X-ray (EDX) spectroscopy was employed in Fig.6, to determine the elemental composition of the biodegradable film surface, conducted via SEM coupled to an EDX detector operating at 15 kV accelerating voltage. The quantitative EDX analysis of Area 561 (magnification 500×) revealed that carbon (C K: 48.7 wt%, 56.3 at.%) and oxygen (O K: 48.6 wt%, 42.2 at.%) together comprised approximately 97.3 wt% of the analyzed material, reflecting a carbohydrate-based polymer matrix characteristic of pectin and its glycosylated derivatives(Mirani et al., 2021). The C/O atomic ratio of 56.3:42.2 (approximately 1.33:1 by molar ratio) is entirely consistent with the theoretical composition of methyl-esterified galacturonic acid units forming the pectin backbone, wherein each sugar residue contains three oxygen atoms per carbon in the backbone plus additional hydroxyl groups and methyl ester functionalities on the side chains, thereby confirming that the film is composed predominantly of bio-derived polysaccharide rather than synthetic polymers or inorganic reinforcing fillers. Minor elemental constituents detected at trace levels (<1.2 at.% each) included fluorine (F K: 1.1 wt%, 0.8 at.%), likely from

polyvinylidene fluoride sample-preparation tape or environmental laboratory contamination; aluminium (Al K: 0.4 wt%, 0.2 at.%) and silicon (Si K: 0.4 wt%, 0.2 at.%), consistent with residual mineral impurities from the banana pseudo-stem feedstock or acid/glass interactions during pectin extraction; sulfur (S K: 0.2 wt%, 0.1 at.%), attributable to residual sulfates from processing; and chlorine (Cl K: 0.5 wt%, 0.2 at.%), derived from residual salts or chlorine-based sanitizers used in feedstock preparation. Notably absent from the EDX spectrum were detectable concentrations of heavy metals, transition metals, or inorganic nanoparticles (ZnO, TiO_2, Al_2O_3, silicates), confirming that the film does not incorporate metallic or ceramic reinforcements and is entirely composed of organic biopolymer without synthetic inorganic additives (Doveri et al., 2025). The elemental homogeneity and uniform distribution across the examined surface area, combined with the absence of phase-segregated domains or particle clustering visible at 500× magnification in the concurrent SEM image, confirms that the film matrix is chemically uniform and purely organic in composition. This all-organic, nanoparticle-free elemental profile is advantageous for food-contact safety, regulatory compliance, and industrial compostability certification, as the material contains no synthetic or persistent inorganic compounds that could leach into food products, compromise environmental degradation in composting environments, or accumulate as persistent microparticles in soil or water systems (Mutalib et al., 2017) (Periyasamy et al., 2025).

3.5.4 Implications for Film Performance and Application

The morphological differences documented through this SEM analysis have direct implications for the functional performance of the prepared biodegradable film. The dense, crack-free, pore-free structure observed in the film indicates superior mechanical integrity compared to a loose aggregate of pectin particles. Films with such homogeneous morphology typically exhibit improved:

Mechanical properties: Tensile strength and elongation at break are enhanced in films with continuous matrices and minimal defects, as stress is distributed more uniformly across the polymer network rather than concentrated at void sites or grain boundaries (Shah et al., 2024).

Barrier properties: The absence of porosity and cracks in the film surface contributes to reduced permeability to gases and moisture, as transport pathways are limited to diffusion through the polymer matrix rather than facilitated by physical defects (Bhatia et al., 2023).

Surface uniformity: The smooth, continuous surface of the film promotes better contact with food surfaces and may enhance adhesion in layered packaging applications.

In contrast, the rough and aggregated nature of the free pectin particles reflects a state in which the polymer has not undergone the geometric reorganization necessary for optimal packing and chain interaction. The substantial surface area of the rough pectin may be advantageous for other applications requiring high reactivity (such as adsorbent materials or emulsifying agents), but is not conducive to film-based packaging applications, where mechanical strength and barrier function depend on polymer chain continuity.

The SEM morphological analysis demonstrates a clear transition from the disordered, particle-aggregate state of extracted pectin to the organized, continuous polymer matrix characteristic of the prepared biodegradable film. This structural reorganization is achieved through the controlled dissolution and solvent-casting process, without the necessity for nanoparticle incorporation. The resulting film exhibits the homogeneous, defect-free morphology consistent with high-performance biopolymer matrices suitable for sustainable food packaging applications. The absence of cracks, pores, and aggregation defects, combined with the dense internal structure visible at high magnification, indicates that the pectin-based film is well-suited for further evaluation of mechanical, thermal, and barrier properties in the context of food storage and preservation applications.

3.6 Evaluation of mechanical, thermal, and barrier properties of developed biodegradable film.

3.6.1 Tensile Strength Performance

The banana pseudo-stem pectin-based biodegradable film exhibited a tensile strength of 1.19 MPa as determined by universal testing machine (UTM) analysis. This value lies within the expected range for highly plasticized pectin films, which typically display tensile strengths between 0.5 and 7.0 MPa depending on formulation parameters including pectin concentration, plasticizer type and loading, and degree of methyl esterification. The measured result reflects the inherent properties of pectin as a soft, hydrophilic polysaccharide with reduced mechanical rigidity compared to synthetic polymers. While unplasticized pectin films demonstrate substantially higher tensile strength (2.49–6.01 MPa), incorporation of plasticizers such as glycerol—necessary for achieving processable films with adequate flexibility—progressively reduces tensile strength through disruption of intermolecular hydrogen bonding (Jantrawut et al., 2017), (Said et al.,2024).

The observed 1.19 MPa suggests a moderate-to-high plasticizer concentration, likely in the 30–40% range by weight, wherein plasticizer molecules intercalate between polymer chains and reduce intermolecular attractive forces. Published data confirm that glycerol-plasticized pectin films experience approximately 39% tensile strength reduction upon increasing plasticizer concentration from 20% to 40%, with values declining from 6.01 MPa to 3.66 MPa. Alternative plasticizers such as propylene glycol or polyethylene glycol at equivalent concentrations yield higher residual tensile strengths (5.11–6.90 MPa), indicating that plasticizer molecular weight and hydrogen-bonding characteristics significantly influence mechanical outcomes and represent optimization opportunities for future formulations (Cabello et al., 2015).

3.6.2 Bursting Strength Performance

The film achieved a bursting strength of 2.75 kg/cm² as measured per ASTM D3786 protocol. Bursting strength quantifies the film's capacity to withstand omnidirectional pressure expansion via diaphragm rupture testing, a metric fundamentally distinct from tensile strength and particularly relevant to food-packaging scenarios involving complex multi-axial loading (Shanbhag et al., 2023). The measured value substantially exceeds reported bursting strengths for pure pectin films (0.036–0.14 kg/cm²) and aligns with moderate-performance biopolymer formulations, indicating functional resistance to radial pressure forces typical in packaging applications (Shanbhag et al., 2023).

The relationship between tensile and bursting strength in plasticized pectin films is not directly proportional; highly plasticized formulations often exhibit lower tensile strength but equal or superior bursting strength due to enhanced elongation capacity and reduced brittleness. The reported 2.75 kg/cm² bursting strength indicates adequate chain entanglement and intermolecular cohesion within the polymer matrix to resist diaphragm-induced rupture, despite the mechanical trade-offs inherent to plasticization. Glycerol incorporation increases film thickness and promotes chain mobility, both of which enhance bursting resistance by enabling controlled deformation before fracture initiation (Bishnoi et al., 2023) (Shanbhag et al., 2023).

3.6.3 Thermogravimetric analysis (TGA) of biodegradable film

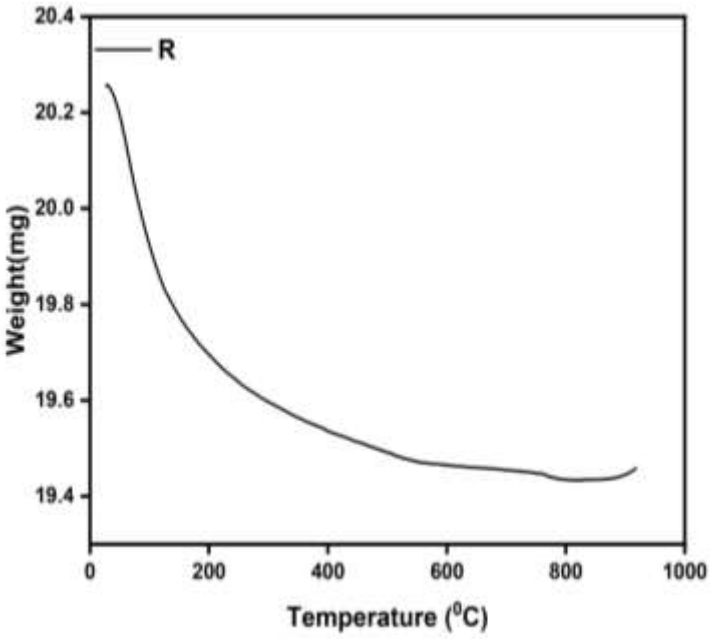

Fig.7, Thermal stability of biodegradable film.

The thermal stability of the banana pseudo-stem pectin biodegradable film was assessed using thermogravimetric analysis (TGA) and differential scanning calorimetry (DSC). In the **Fig.7**, the TGA curve represents the sample mass decreased only slightly from about 20.3 mg at room temperature to roughly 19.45 mg at 1000°C, corresponding to an overall mass loss of around 4%, which shows that the film forms a relatively stable carbonaceous residue rather than undergoing complete volatilisation (Asfaw et al., 2023). The first decrease in mass occurred below about 120°C and can be attributed to evaporation of bound water and low-molecular-weight volatiles trapped in the hydrophilic pectin network (R et al., 2023). The main weight-loss region between roughly 120 and 350°C reflects breakdown of the galacturonic-acid backbone and side groups together with the thermal decomposition of glycerol, which is consistent with the broad primary degradation range reported for highly plasticized pectin films and supports the inference that this formulation contains a relatively high plasticizer fraction (Dambuza et al., 2024). Beyond about 350°C the rate of mass loss slowed markedly, indicating gradual oxidation of more condensed carbon structures, and above roughly 600°C the mass approached a plateau, suggesting the presence of thermally stable mineral residues originating from the pseudo-stem feedstock or processing aids (Cabello et al., 2015).

3.6.4 Differential Scanning Calorimetry (DSC) analysis of biodegradable film.

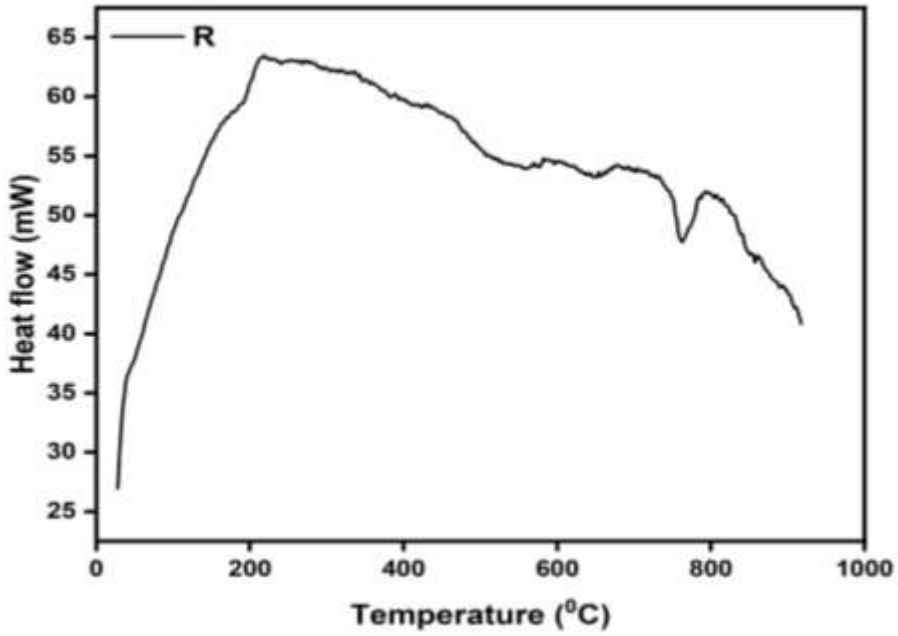

Fig.8, Differential Scanning Calorimetry (DSC) analysis of biodegradable film.

The DSC trace complements the TGA results by clarifying the energetic nature of these transitions. A broad endothermic region between about 100 and 200°C, with a shallow minimum in the vicinity of 140–160°C, is consistent with energy uptake associated with desorption of water and with the glass-transition region of an amorphous, glycerol-rich pectin matrix; the breadth and low intensity of this feature match literature reports where 30–40% glycerol depresses the pectin glass-transition temperature into a wide, ill-defined interval instead of a sharp step(R et al., 2023). The dominant event in **Fig.8,** the DSC curve is a strong exothermic peak centred near 310°C that coincides with the main TGA mass-loss zone and can be associated with oxidative degradation of the polysaccharide backbone and combustion of the glycerol plasticizer, a behaviour typical of pectin systems in which high chain mobility accelerates decomposition once critical bond scission begins (Dambuza et al., 2024). Smaller exothermic fluctuations at higher temperatures likely arise from oxidation of partially carbonised residues, and the eventual return of the heat-flow signal towards baseline above about 550°C indicates that all energetically significant decomposition processes are complete by this stage, leaving only inorganic ash (Asfaw et al., 2023).

Taken together, the TGA and DSC data show that the film remains thermally stable across all expected storage conditions and under moderate processing temperatures but begins to degrade rapidly when exposure exceeds about 150–180°C, which is consistent with the high level of plasticization implied by the relatively low tensile strength and good flexibility measured for this material (Syarifuddin et al., 2025). This thermal profile is advantageous for ambient and chilled food-packaging uses, where the material will not approach its decomposition range, but it also indicates that high-temperature operations such as retort sterilisation or prolonged extrusion must be avoided unless the plasticizer content is reduced or replaced with thermally more robust additives (Asfaw et al., 2023) (Dambuza et al., 2024).

3.7 Soil Biodegradation analysis of biodegradable film.

The biodegradation behaviour of the pectin-based biodegradable film was evaluated by monitoring weight loss over a period of 90 days, using an initial sample weight of 5 g. The percentage weight loss at different degradation intervals is presented in Table 1 and illustrated in Figure 9.

Sl.no.	No. of days.	Weight Loss(gm) Total=5gm	Weight loss (%)
1	15	4.8	96
2	30	3.7	74
3	45	2.6	52
4	60	1.9	38
5	75	0.8	16
6	90	0.1	2

The percentage weight loss is calculated using:

$$\text{Weight loss (\%)} = \frac{\text{Weight loss (g)}}{5\text{ g}} \times 10$$

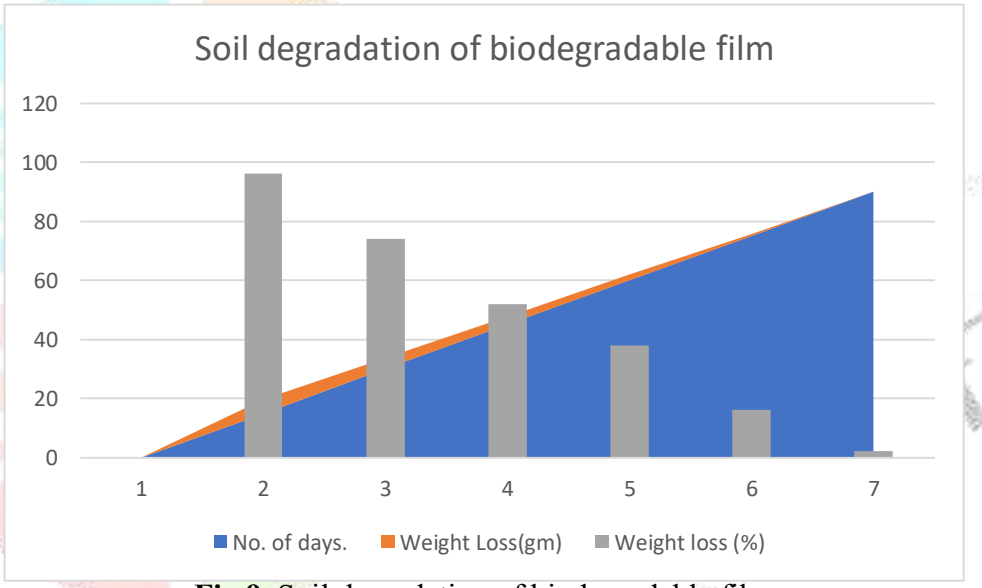

Fig.9, Soil degradation of biodegradable film

The results indicate a rapid initial degradation, with the film exhibiting 96% weight loss within the first 15 days, suggesting high susceptibility of the pectin matrix to microbial and environmental action. This rapid mass reduction can be attributed to the hydrophilic nature of pectin and the presence of readily biodegradable polysaccharide chains, which facilitate water absorption and microbial colonization.

As the degradation period progressed, the rate of weight loss gradually decreased. At 30 and 45 days, the film showed 74% and 52% weight loss, respectively, indicating continued breakdown of the polymer network. The slower degradation observed after 45 days may be due to the depletion of easily degradable components, leaving behind more structurally stable fractions.

By 60 and 75 days, the weight loss further declined to 38% and 16%, demonstrating the gradual mineralization of the remaining polymer matrix. At the end of 90 days, only 2% residual mass remained, confirming the near-complete biodegradation of the film. Overall, the degradation profile confirms that the developed pectin-based film exhibits excellent biodegradability, making it a promising candidate for eco-friendly and sustainable packaging applications, where rapid environmental breakdown is desirable.

3.8 Conclusion

In the present study, biodegradable films were successfully developed from pectin extracted from banana pseudostem waste, demonstrating the effective valorization of an abundant agro-industrial by-product. The extraction process yielded pectin with suitable functional characteristics for film formation, confirming banana pseudostem as a viable alternative source of pectin. The prepared pectin-based films exhibited good film-forming ability, uniform appearance, and satisfactory mechanical integrity, indicating their potential applicability in biodegradable packaging systems.

References

- Agarwal, N., Jyoti, N., Thakur, M., Mishra, B. B., & Singh, S. P. (2023). Preparation and characterization of biodegradable films based on levan polysaccharide blended with gellan gum. *Environmental Technology & Innovation*, *31*, 103231. https://doi.org/10.1016/j.eti.2023.103231
- Arias, D., Rodríguez, J., López, B., & Méndez, P. (2021). Evaluation of the physicochemical properties of pectin extracted from Musa paradisiaca banana peels at different pH conditions in the formation of nanoparticles. *Heliyon*, *7*(1), e06059. https://doi.org/10.1016/j.heliyon.2021.e06059
- Asfaw, W. A., Tafa, K. D., & Satheesh, N. (2023). Optimization of citron peel pectin and glycerol concentration in the production of edible film using response surface methodology. *Heliyon*, *9*(3), e13724. https://doi.org/10.1016/j.heliyon.2023.e13724
- Benmebarek, I. E., Gonzalez-Serrano, D. J., Aghababaei, F., Ziogkas, D., Garcia-Cruz, R., Boukhari, A., Moreno, A., & Hadidi, M. (2024). Optimizing the microwave-assisted hydrothermal extraction of pectin from tangerine by-product and its physicochemical, structural, and functional properties. Food Chemistry: X, 23, 101615. https://doi.org/10.1016/j.fochx.2024.101615
- Bhatia, S., Al-Harrasi, A., Alhadhrami, A. S., Shah, Y. A., Kotta, S., Iqbal, J., Anwer, M. K., Nair, A. K., Koca, E., & Aydemir, L. Y. (2023). Physical, Chemical, Barrier, and Antioxidant Properties of Pectin/Collagen Hydrogel-Based Films Enriched with Melissa officinalis. *Gels*, *9*(7), 511. https://doi.org/10.3390/gels9070511
- Bishnoi, A., Chandla, N. K., Talwar, G., Khatkar, S. K., & Sharma, A. (2023). Mechanical strength, solubility, and functional studies of developed composite biopolymeric film. *Journal of Food Processing and Preservation*, *2023*, 1–19. https://doi.org/10.1155/2023/5108490
- Cabello, S. P., Takara, E., Marchese, J., & Ochoa, N. (2015). Influence of plasticizers in pectin films: Microstructural changes. *Materials Chemistry and Physics*, *162*, 491–497. https://doi.org/10.1016/j.matchemphys.2015.06.019
- Dambuza, A., Rungqu, P., Oyedeji, A. O., Miya, G. M., Kuria, S. K., Hosu, S. Y., & Oyedeji, O. O. (2024). Extraction, Characterization, and Antioxidant Activity of Pectin from Lemon Peels. *Molecules*, *29*(16), 3878. https://doi.org/10.3390/molecules29163878
- Davoodi, M. N., Milani, J. M., & Farahmandfar, R. (2021). Preparation and characterization of a novel biodegradable film based on sulfated polysaccharide extracted from seaweed Ulva intestinalis. *Food Science & Nutrition*, *9*(8), 4108–4116. https://doi.org/10.1002/fsn3.2370
- Doveri, L., Fernandez, Y. a. D., Dacarro, G., Grisoli, P., Milanese, C., Urena, M., Sok, N., Karbowiak, T., & Pallavicini, P. (2025). Active Pectin/Carboxymethylcellulose composite films for bread packaging. *Molecules*, *30*(11), 2257. https://doi.org/10.3390/molecules30112257
- Farris, S., & Scandola, M. (2022). Tailoring the barrier and mechanical properties of polysaccharide-based films for food packaging. Food Packaging and Shelf Life, 31, 100792. https://doi.org/10.1016/j.fpsl.2021.100792
- Fu, X., Chang, X., Ding, Z., Xu, H., Kong, H., Chen, F., Wang, R., Shan, Y., & Ding, S. (2022). Fabrication and characterization of Eco-Friendly polyelectrolyte bilayer films based on chitosan and different types of edible citrus pectin. *Foods*, *11*(21), 3536. https://doi.org/10.3390/foods11213536

- Hosseini, S. S., Khodaiyan, F., & Yarmand, M. S. (2015). Optimization of microwave assisted extraction of pectin from sour orange peel and its physicochemical properties. *Carbohydrate Polymers*, *140*, 59–65. https://doi.org/10.1016/j.carbpol.2015.12.051 (Hosseini et al., 2015)
- Hussain, S., Rehman, A., Sohail, M., & Qamar, S. A. (2022). Extraction and characterization of pectin from agro-industrial wastes and its application in biodegradable films: A review. International Journal of Biological Macromolecules, 222, 1531-1543. https://doi.org/10.1016/j.ijbiomac.2022.09.235
- Jantrawut, P., Chaiwarit, T., Jantanasakulwong, K., Brachais, C., & Chambin, O. (2017). Effect of plasticizer type on tensile property and in vitro indomethacin release of thin films based on Low-Methoxyl pectin. *Polymers*, *9*(7), 289. https://doi.org/10.3390/polym9070289
- Jiang, Y., & Du, J. (2016). Properties of high-methoxyl pectin extracted from "Fuji" apple pomace in China. *Journal of Food Process Engineering*, *40*(3). https://doi.org/10.1111/jfpe.12497
- Kezer, G., Yusufoğlu, B., Namlı, S., Zhao, T., Ziora, Z. M., & Esatbeyoglu, T. (2025). A green sustainable insight for waste management: Recycling of banana peel as a functional ingredient. *Applied Food Research*, *5*(2), 101421. https://doi.org/10.1016/j.afres.2025.101421 (Kezer et al., 2025)
- Kumar, A., Chauhan, G. S., & Sharma, R. (2024). Role of plasticizers and drying conditions on the crystallinity and performance of biopolymer films. Carbohydrate Polymer Technologies and Applications, 7, 100419. https://doi.org/10.1016/j.carpta.2024.100419
- Kyomugasho, C., Christiaens, S., Shpigelman, A., Van Loey, A. M., & Hendrickx, M. E. (2014). FT-IR spectroscopy, a reliable method for routine analysis of the degree of methylesterification of pectin in different fruit- and vegetable-based matrices. *Food Chemistry*, *176*, 82–90. https://doi.org/10.1016/j.foodchem.2014.12.033
- Lal, S., Kumar, V., & Arora, S. (2020). Eco-friendly synthesis of biodegradable and high strength ternary blend films of PVA/starch/pectin: Mechanical, thermal and biodegradation studies. *Polymers and Polymer Composites*, *29*(9), 1505–1514. https://doi.org/10.1177/0967391120972881
- Li, K., Jin, S., Liu, X., Chen, H., & He, J. (2023). Preparation and characterization of chitosan/pectin composite films with enhanced mechanical and barrier properties. Polymers, 15(4), 850. https://doi.org/10.3390/polym15040850
- Mao, Y., Dewi, S. R., Harding, S. E., & Binner, E. (2024). Influence of ripening stage on the microwave-assisted pectin extraction from banana peels: A feasibility study targeting both the Homogalacturonan and Rhamnogalacturonan-I region. Food Chemistry, 460, 140549. https://doi.org/10.1016/j.foodchem.2024.140549
- Mirani, F., Maffini, A., Casamichiela, F., Pazzaglia, A., Formenti, A., Dellasega, D., Russo, V., Vavassori, D., Bortot, D., Huault, M., Zeraouli, G., Ospina, V., Malko, S., Apiñaniz, J. I., Pérez-Hernández, J. A., De Luis, D., Gatti, G., Volpe, L., Pola, A., & Passoni, M. (2021). Integrated quantitative PIXE analysis and EDX spectroscopy using a laser-driven particle source. *Science Advances*, *7*(3). https://doi.org/10.1126/sciadv.abc8660
- Moso, T. N., Pillai, C. K. S., & Ray, S. S. (2023). Structural insights into pectin-based biomaterials: From extraction to application. Materials Today Communications, 34, 105193. https://doi.org/10.1016/j.mtcomm.2022.105193
- Mutalib, M. A., Rahman, M., Othman, M., Ismail, A., & Jaafar, J. (2017). Scanning electron microscopy (SEM) and Energy-Dispersive X-Ray (EDX) spectroscopy. In *Elsevier eBooks* (pp. 161–179). https://doi.org/10.1016/b978-0-444-63776-5.00009-7
- Muthiah, P. L., & Ching, Y. C. (2023). Recent advances in pectin extraction, characterization, and pectin-based film applications. Journal of Polymers and the Environment, 31(3), 839-876. https://doi.org/10.1007/s10924-022-02624-w

- Periyasamy, T., Asrafali, S. P., & Lee, J. (2025). Recent Advances in Functional Biopolymer Films with Antimicrobial and Antioxidant Properties for Enhanced Food Packaging. *Polymers*, *17*(9), 1257. https://doi.org/10.3390/polym17091257
- Phaiphan, A., Churat, S., Dougta, T., Wichalin, P., Khanchai, W., & Penjumras, P. (2020). Effects of microwave and ultrasound on the extraction of pectin and its chemical characterisation of banana (Musa sapientum L.) peels. Food Research, 4(6), 2030–2036. https://doi.org/10.26656/fr.2017.4(6).248
- R, S. M., M, R. K., S, B., B, H. A., Vishwanath, P. M., Syed, A., Eswaramoorthy, R., Amachawadi, R. G., Shivamallu, C., Chattu, V. K., Majani, S. S., & Kollur, S. P. (2023). Pectin/PVA and pectin-MgO/PVA films: Preparation, characterization and biodegradation studies. *Heliyon*, *9*(5), e15792. https://doi.org/10.1016/j.heliyon.2023.e15792
- Rajendran, N., & Thampi, B. H. (2019). EXTRACTION AND CHARACTERISATION OF PECTIN FROMBANANA PEEL. *Carpathian Journal of Food Science and Technology*, 45–63. https://doi.org/10.34302/2019.11.4.4
- Ren, W., Qiang, T., & Chen, L. (2022). Recyclable and biodegradable pectin-based film with high mechanical strength. *Food Hydrocolloids*, *129*, 107643. https://doi.org/10.1016/j.foodhyd.2022.107643 (Ren et al., 2022)
- Rivadeneira, J. P., Wu, T., Ybanez, Q., Dorado, A. A., Migo, V. P., Nayve, F. R. P., & Castillo-Israel, K. A. T. (2020). Microwave-Assisted Extraction of Pectin from "Saba" Banana Peel Waste: Optimization, Characterization, and Rheology Study. International Journal of Food Science, 2020, 1–9. https://doi.org/10.1155/2020/8879425
- Riyamol, N., Chengaiyan, J. G., Rana, S. S., Ahmad, F., Haque, S., & Capanoglu, E. (2023). Recent Advances in the Extraction of Pectin from Various Sources and Industrial Applications. *ACS Omega*, *8*(49), 46309–46324. https://doi.org/10.1021/acsomega.3c04010
- Said NS, Olawuyi IF, Lee WY. Tailoring Pectin-PLA Bilayer Film for Optimal Properties as a Food Pouch Material. Polymers (Basel). 2024 Mar 5;16(5):712. doi: 10.3390/polym16050712. PMID: 38475392; PMCID: PMC10933983.
- Sarah, M., Hasibuan, I. M., Misran, E., & Maulina, S. (2022). Optimization of Microwave-Assisted Pectin Extraction from Cocoa Pod Husk. Molecules, 27(19), 6544. https://doi.org/10.3390/molecules27196544
- Serrafi, A., Wikiera, A., Cyprych, K., & Malik, M. (2025). Spectroscopic and microscopic analysis of apple pectins. *Molecules*, *30*(7), 1633. https://doi.org/10.3390/molecules30071633
- Shah, Y. A., Bhatia, S., Chinnam, S., Al-Harrasi, A., Tarahi, M., Khan, T. S., Alam, T., Koca, E., Aydemir, L. Y., Philip, A. K., Afzaal, M., Khan, M. R., & Pratap-Singh, A. (2024). Myrrh Oleo-Gum resin as a functional additive in pectin and K-Carrageenan composite films for food packaging. *Food Science & Nutrition*, *12*(12), 10284–10295. https://doi.org/10.1002/fsn3.4524
- Shanbhag, C., Shenoy, R., Shetty, P., Srinivasulu, M., & Nayak, R. (2023). Formulation and characterization of starch-based novel biodegradable edible films for food packaging. *Journal of Food Science and Technology*, *60*(11), 2858–2867. https://doi.org/10.1007/s13197-023-05803-2
- Sharma, S., & Wadhwa, N. (2023). Extraction of Pectin from Banana Pseudo Stem. *Current Trends in Biotechnology and Pharmacy*, *17*(4), 1390–1398. https://doi.org/10.5530/ctbp.2023.4.73
- Syarifuddin, A., Muflih, M. H., Izzah, N., Fadillah, U., Ainani, A. F., & Dirpan, A. (2025). Pectin-based edible films and coatings: From extraction to application on food packaging towards circular economy- A review. *Carbohydrate Polymer Technologies and Applications*, *9*, 100680. https://doi.org/10.1016/j.carpta.2025.100680
- Zhou, Y., Wu, Z., & Dai, J. (2022). Crystallization behavior of biopolymer films during solvent casting: Mechanisms and implications. Progress in Organic Coatings, 172, 107089. https://doi.org/10.1016/j.porgcoat.2022.107089

- Zhu, Y., Liu, K., Yuen, M., Yuen, T., Yuen, H., & Peng, Q. (2022). Extraction and characterization of a pectin from sea buckthorn peel. *Frontiers in Nutrition*, *9*, 969465. https://doi.org/10.3389/fnut.2022.969465